Available online at www.sciencedirect.com

ScienceDirect

Procedia - Social and Behavioral Sciences 108 (2014) 296 – 305

Procedia
Social and Behavioral Sciences

AIRO Winter 2013

Geometric and computational models of chromatin fibre folding for human embryonic stem cells

Francesca Maggioni[a,*], Marida Bertocchi[a], Ettore Mosca[b], Rolland Reinbold[b] and Ileana Zucchi[b]

[a] *Department of Management, Economics and Quantitative Methods, University of Bergamo, Italy*
[b] *Institute of Biomedical Technologies, ITB-CNR, Segrate Milan, Italy*

Abstract

In this study we analyze the chromatin state of human pluripotent stem cells by geometric and computational modelling of fibre conformation. The model takes into account local structure of chromatin organized into euchromatin, permissive for gene activation, and heterochromatin, transcriptionally silenced. Euchromatin was modelled using linear DNA while heterochromatin by means of a solenoid structure in which DNA winds onto six nucleosome spools per turn. Two geometric models are presented and are compared in terms of geometric quantities. The models are tested using in vivo data generated from chromatin human immunoprecipitation from embryonic stem cells. This study provides insight for identifying the relationships between chromosome geometry and epigenomic processes associated with chromatin remodeling, cellular reprograming and maintenance of cellular pluripotency.

Keywords: chromatin structure; pluripotency; epigenomics; geometric modelling; euchromatin; heterochromatin.

1. Introduction

The human genome is estimated to contain approximately 30,000 unique genes. Though every gene exists within every cell in the human body, only a small percentage of these genes is active in any given cell. What promotes the transcription of cell-specific genes and determines the cell identity? Chromatin structure and its ability for remodeling into different states.

Recent data show that stem cell chromatin differs from that of somatic or differentiated cells in several structural and functional aspects, such as global chromatin arrangement, condensation and compaction. Moreover,

* Corresponding author: Tel.: +39-035-2052649 ; fax: +39-035-2052549

E-mail address: francesca.maggioni@unibg.it

doi:10.1016/j.sbspro.2013.12.839

undifferentiated embryonic stem (ES) cells are characterized by hyperdynamic plasticity of chromatin proteins, supporting an open conformation model of chromatin in undifferentiated stem cells. Hence, chromatin state is currently being considered as one of the most important factors for self-renewal and pluripotency of ES cells. The chromatin state of a cell is defined through the establishment and the maintenance of localized open and closed states of the chromatin structure, determined by epigenomic interactors.
In fact mutations in epigenomic regulators have the potential to alter the chromatin structure, leading to mis-regulation of gene expression and contribute to cancer or other diseases.
Therefore understanding chromatin remodeling is of fundamental significance in understanding cancer and for regenerative medicine.
The focus of our research is on identifying and characterizing the chromatin state of Pluripotent Stem Cells (PSCs). PSCs are characterized by extensive self-renewal and multi-lineage differentiation potential. PSCs generate all functional tissues of the body during development and adult stem cells (SCs) that allow for regeneration of these tissues following injury or degenerative processes. In this study we present a summary of an extensive analysis on the chromatin state using in vivo data generated from chromatin immunoprecipitation of human embryonic stem cells with Oct4, Sox2 and Nanog transcription factors. The investigation is carried out using geometrical and computational models of the chromatin fibre conformation.

2. Measures and energetics of filament coiling

In this section we show how to investigate several geometric features of the DNA filament, such as writhing, inflexional configuration, torsion and twist localization, in relation to properties of physical interest, such as elastic deformation energy and filament compaction (Maggioni & Ricca, 2006; Ricca & Maggioni, 2008; Maggioni, Potra & Bertocchi, 2013, Maggioni, Alamri, Barenghi & Ricca 2013).
For this purpose we refer to an inextensible, smooth, simple closed curve C in the three-dimensional space $\mathbb{R}^3$, thought of as the central axis of a closed, double-stranded DNA filament. Each point on C is labeled by the position vector $\mathbf{X}=\mathbf{X}(\xi)$, where $\xi\in[0, L_{fin}]$, its curvature by $c(\xi)$, torsion $\tau(\xi)$ and $\hat{\mathbf{t}} = \dfrac{\mathbf{X}'(\xi)}{\left\| \mathbf{X}'(\xi) \right\|}$ the unit tangent to C at ξ and $l(\xi)$ the length function.
Coiling is measured by the *normalized total curvature* of C that is given by

$$\mathcal{K} := \frac{1}{l(\xi)} \int_0^{L_{fin}} c(\xi) \left\| \mathbf{X}'(\xi) \right\| \mathrm{d}\xi.$$

The folding process conserves topology. For a thin filament this means conservation of the linking number Lk (Călugăreanu, 1961; White, 1969), given by

$$Lk := Wr + Tw\,,$$

where Wr represents the *writhing number* (Fuller, 1971) and Tw represents the total twist of the filament fibres. These are assumed to be wound uniformly around the axis C.
Denoting by $\Omega = \Omega(\xi)$ the angular twist rate of the fibres, we have that the *normalized total twist* is given by

$$Tw := \frac{1}{l(\xi)} \left(\frac{1}{2\pi} \int_0^{L_{fin}} \Omega(\xi) \left\| \mathbf{X}'(\xi) \right\| \mathrm{d}\xi \right),$$

which is related to the geometry of the filament axis through the decomposition

$$Tw := \frac{1}{l(\xi)} \left(\frac{1}{2\pi} \int_0^{L_{fin}} \tau(\xi) \left\| \mathbf{X}'(\xi) \right\| \mathrm{d}\xi + \frac{1}{2\pi} [\Theta]_{\mathcal{F}} \right),$$

where the first term in the r.h.s. is the normalized total torsion $\mathcal{T}$ and the second term is the normalized intrinsic twist $\mathcal{N}$ of the fibres *around C*.

In terms of deformation energy, the process of folding and coiling of DNA filaments due to the relaxation of high twist is characterized by a transfer of torsional energy to bending energy. To analyze the energetics of folding we consider the DNA filament modeled by a thin, inextensible rod, of uniform circular cross-section of area $A = \pi a^2$ centered on *C* and radius $a = 1$ *nm*.

The elastic characteristics are specified by the bending rigidity K_b and the torsional rigidity K_t of the filament. In general $\chi \in [1,1.5]$, with $\chi = \frac{K_b}{K_t}$. The stress-strain relation leads to the conventional quadratic form of the deformation energy, given by

$$E := E_b + E_t = \frac{1}{l(\xi)} \int_0^{L_{fin}} \left[K_b (c(\xi))^2 + K_t (\Omega(\xi))^2 \right] \left\| \mathbf{X}'(\xi) \right\| \mathrm{d}\xi,$$

where we assumed a zero natural twist rate of the filament fibres, an usual assumption for the relaxed configuration (Maggioni & Ricca, 2006). The deformation energy E is thus given by the sum of the bending energy E_b due to curvature effects, and the torsional energy E_t, due to torsion and intrinsic twist.

3. Geometric models of the 30nm chromatin fibre

In eukaryotes, the DNA is organized in a chromatin fibre, a complex made of DNA wrapped around a core histone octamer, which consists of histones of 2 copies each of H2A, H2B, H3, H4. The chromatin building block is the nucleosome. In the core particle, 147 base pairs (*bp*) are wrapped in 1.7 left-handed superhelical turns around the histone octamer. Each nucleosome core is connected by a *linker* DNA to make repetitive motifs so the fibre forms a "beads-on-a-string" like model (Olins & Olins, 2003).

More than 30 years ago, Finch and Klug first proposed that the nucleosome is folded into 30-nm chromatin fibres (Finch & Klug, 1976).

The detailed structure of the chromatin fibre has remained controversial for over three decades (Van Holde & Zlatanova, 2007, Tremethick, 2007), with evidence supporting both zig-zag ("two-start") (Doringo et al., 2004; Schalch et al., 2005; Worcel et al., 1981) and solenoid ("one-start") (Finch & Klug, 1976) models coming from various sources, including X-ray crystallography and electron microscopy. In the solenoid model, consecutive nucleosomes are located next to each other in the fibre, folding into a simple one-star helix. Subsequently, a second model of the two-start helix was proposed on the basis of microscopic observations of isolated nucleosomes, where a nucleosome in the fibre is bound to the second neighbor but not the first.

Over several years, chromatin models have been designed in increasing level of detail, each of which is suitable for certain biological problems and applications. The first-generation "macroscopic" models treated the nucleosome and the wound DNA according to general mechanical and electrostatic properties, with the histone tails approximated as rigid bodies and linker histones neglected (Beard & Schlick, 2001a; 2001b; 2003; Zhang, Beard & Schlick, 2003; Sun, Zhang & Schlick, 2005). It captured the fundamental monovalent-salt dependent mechanics of chromatin and the thermal fluctuations of the nucleosome and linker DNA.

Chromatin has finally been crystallized, providing some measurements on the way DNA is wrapped around an octamer.

We will restrict our study on the basis of geometry without introducing any kind of interaction. We will use the general assumption that the local structure of the chromatin is periodical such that each pattern has exactly the same environment (Schiessel, 2013). We assume that there are six nucleosomes per turn in the solenoid with each nucleosome radius $r = 5.5$ *nm,* and a wrapping angle of the DNA molecule around a nucleosome given by $\theta = 3.5\ \pi$, shaped into a helix with a pitch of $P = 2.8$ *nm* and with a nucleosome wrapping length:

$\Lambda = \theta\sqrt{r^2 + \frac{P^2}{4\pi^2}} \approx 5.5\,nm$ around 147 bp (Finch & Klug, 1976). The connection between two nucleosomes is described by a linker-DNA of length b = 50 *bp*. The quantity $L = \Lambda + b = 197\,bp$ is referred to as the *repeat length* and a value of 200 *bp* is often considered to be realistic (Rossetto & Evaraers, 2005; Woodcock et al. 1993), see in Table 1 a summary of the values of the models parameters.
We introduce now two geometric models for a single solenoid turn: the *six helices model* and the *torus unknot model*.

Table 1. Summary of the values of the model parameters.

A	*R*	*R*	*θ*	*P*	Λ	*B*	*L*=Λ+*b*	*S*	*Q*
1 nm	*5.5 nm*	*9.5*	*3.5 π*	*2.8 nm*	*5.5 nm*	*50 bp*	*197 bp*	*1*	*12*

3.1 Six helices model for a solenoid turn (Heterochromatin)
Assigning a number i = 0,…,5 to the i−nucleosomes which belong to a single solenoid turn, the following parametric equation $\mathbf{X}_i(\xi)$ represents the DNA filament wrapped around the corresponding nucleosome i = 0,…,5 (see Fig. 1(a)), where the parameter $i(2\pi) \le \xi \le (i+1)2\pi$ parameterizes the points of the curve along its length:

$$\mathbf{X}_i := \begin{cases} x = \dfrac{\pi\left(P - 2r\sin\left(\frac{1}{6}(2\pi i + \pi)\right)\cos(\theta(\xi - 4\pi i))\right) + P(-4\pi i + \xi - \pi)\cos\left(\frac{1}{6}(2\pi i + \pi)\right) + 2\pi R\cos\left(\frac{1}{3}\pi(i-1)\right)}{2\pi} \cdot \dfrac{\Lambda}{l(\xi)} \\ y = \dfrac{P(-4\pi i + \xi - \pi)\sin\left(\frac{1}{6}(2\pi i + \pi)\right) + 2\pi r\cos\left(\frac{1}{6}(2\pi i + \pi)\right)\cos(\theta(\xi - 4\pi i)) + 2\pi R\sin\left(\frac{1}{3}\pi(i-1)\right)}{2\pi} \cdot \dfrac{\Lambda}{l(\xi)} \\ z = r\sin(\theta(\xi - 4\pi i)) \cdot \dfrac{\Lambda}{l(\xi)} \end{cases}$$

and where, in order to ensure inextensibility, each component has been normalized by the length function

$$l(\xi) = \int_0^{L_{fin}} \left[\left(\frac{\partial x}{\partial \xi}\right)^2 + \left(\frac{\partial y}{\partial \xi}\right)^2 + \left(\frac{\partial z}{\partial \xi}\right)^2\right]^{\frac{1}{2}} \mathrm{d}\xi.$$

This re-scaling ensures that the total length is kept fixed at Λ =147 *bp*. (for further details see Dorigo et al., 2004). Parameters P, θ, and r are defined as above and R = 9.5 *nm* such that $R + r$ = *15 nm*.
Connections $\mathbf{Y}_i(\xi)$, between two successive nucleosomes (DNA linkers) are approximated by a cubic Hermite spline interpolation (de Boor, 1978), a particular class of a third-degree spline interpolation with each polynomial of the spline in *Hermite form*, which consists of two control points and two control tangents for each polynomial. For a detailed description of the mathematical model in Hermite form adopted to describe DNA linkers we refer to Maggioni et al. (in preparation). A single turn of the six helices model composed by the 6 helices $\mathbf{X}_0$, $\mathbf{X}_1$, $\mathbf{X}_2$, $\mathbf{X}_3$, $\mathbf{X}_4$, $\mathbf{X}_5$, the connections between two successive nucleosomes $\mathbf{Y}_0$, $\mathbf{Y}_1$, $\mathbf{Y}_2$, $\mathbf{Y}_3$, $\mathbf{Y}_4$ and the connection $\mathbf{Y}_5$ with the next solenoid layer is displayed in Fig. 1(a).

3.2 Torus unknot model for a solenoid turn (Heterochromatin)

We propose another model for a single solenoid layer. Let $\mathbf{Z}_i(\xi)$ represents an open *Fourier torus unknot* (Kauffman, 1997), where $i(2\pi) \le \xi \le (i+1)2\pi - h$, $i = 0,...,N-1$, is a parameter along the curve, N the total number of solenoid turns and h a small value in order to leave the curve open and to be connected with the next solenoid turn.

$$\mathbf{Z}_i(\xi) := \begin{cases} x = \cos(\xi)\left(R + r\cos\left[\left(\frac{Q}{P}\right)\xi\right]\right)(6L-b)/l(\xi) \\ y = \sin(\xi)\left(R + r\cos\left[\left(\frac{Q}{P}\right)\xi\right]\right)(6L-b)/l(\xi) \\ z = r\sin\left[\left(\frac{Q}{P}\right)\xi\right](6L-b)/l(\xi) \end{cases}$$

The DNA filament winds around a torus S-times (S = 1) in the longitudinal direction and Q-times (Q = 12) in the meridian direction so to have 2 turns per nucleosome (see Fig.1(b)).
In order to ensure inextensibility, each component has been normalized by the length function $l(\xi)$ where its length is fixed at $6L$ - b=1132 *bp* and r and R chosen as above.
The i-turn $\mathbf{Z}_i$ (ξ) of the solenoid finally is connected with the (i+1)-turn $\mathbf{Z}_{i+1}$ (ξ) by means of cubic Hermite spline functions of length b. An example of the final solenoid structure composed by 10 turns is shown in Fig. 2. Fig. 1(a)-(b) and 2 have been obtained under the Mathematica 9 environment by using the formulas described in Sections 3.1 and 3.2 and the cubic Hermite spline interpolation for the linkers between nucleosomes.

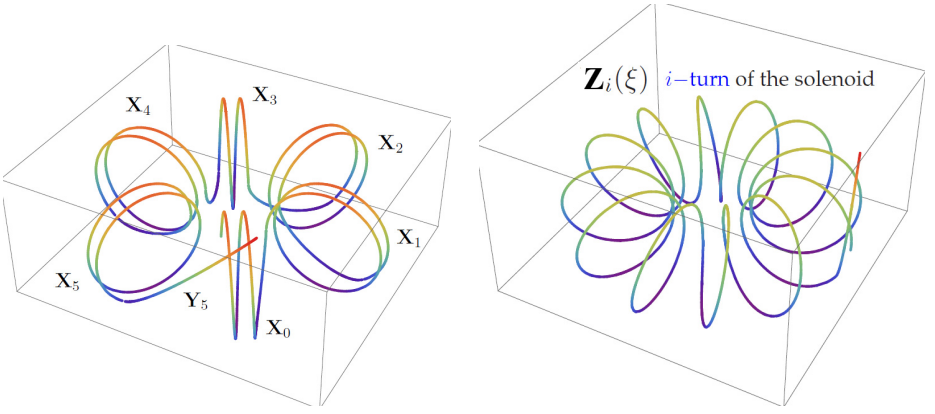

(a) (b)

Fig. 1. (a) Side view of a single turn of the six helices model composed by the 6 helices with a parametric equation $\mathbf{X}_0$, $\mathbf{X}_1$, $\mathbf{X}_2$, $\mathbf{X}_3$, $\mathbf{X}_4$, $\mathbf{X}_5$, the connections between two successive nucleosomes and the connection $\mathbf{Y}_5$ with the next solenoid layer. (b) Side view of a single turn of the *torus unknot model* composed of 12 turns in the meridian direction and one in the longitudinal direction. The connection with the next solenoid layer is also shown.

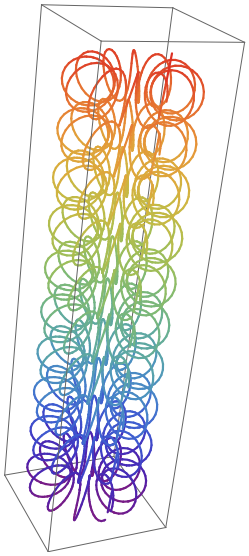

Fig. 2. Example of the solenoid model (10 turns).

4. Numerical results (ChIP Data Analysis)

To study the chromatin state of PSCs we utilize extensive ChIP (Chromatin ImmunoPrecipitation) data generated from native pluripotent human embryonic stem cells (ESCs) (Boyer et al., 2005). ChIP experiments were performed with antibodies specifically against Oct4, Sox2 and Nanog, transcription factors (TFs) important for maintaining the pluripotential state. ChIP analysis was used to identify binding sites for Oct4, Sox2 and Nanog transcription factors on all chromosomes. Recently it was demonstrated that Oct4 alone, or Oct4, Sox2 and Klf4 in combination were sufficient to induce the pluripotent state and generate iPSCs (induced pluripotent stem cells) from various types of cells of the human and mouse body (Boyer et al., 2005; Kim et al., 2009a; Kim et al., 2009b; Takahashi & Yamanaka 2006; Wernig et al., 2007; Zhou et al., 2012; Aoi et al., 2008; Melton et al., 2005). The iPSCs are generated by, local and/or global chromatin structural changes that result in chromatin remodeling induced by these transcription factors binding to particular regions of the chromosomes. ChIP analysis generates local and global pictures of the chromosome structure of iPSCs. Structural changes can be investigated at different time points during cellular reprogramming since changes are maintained for analysis by a chemical cross-linking step utilized with ChIP. Following crosslinking, chromatin is sheared and immunoprecipitation is performed resulting in the purification of protein DNA complexes. DNA sequencing or microarray analysis identify on the chromosomes where the protein binds on a genome-wide scale.

We have developed an algorithm to analyze the chromatin structure and therefore state of human pluripotent cells, based on the observation that Oct4, Sox2 and Nanog are sufficient to initiate a cascade of histone protein modifications that result in an epigenomically induced permanent change of cell state, a process called cell transdifferentiation. Regions where Oct4, Sox2 and Nanog bind we conjecture are sites in which the chromosome are more responsive to, and therefore in a more open state for transcription. Analyzing approximately 3000 chromosome regions bound by Oct4, Nanog and Sox2 proteins, the algorithm looks for the open regions by taking into account the genes which appear within 8kb upstream and downstream of each transcription start site, the distance of each gene from the transcription start site and the length of structural genes. The algorithm matches the zones bound by at least one transcription factor by an appropriate ordering and it has been developed under EXCEL 2010 environment. The length of the closed region of a chromosome is obtained by difference of

the total length of the chromosome and the open region obtained by the procedure explained above. Fig. 3 represents the ratio between closed versus open base pair regions over all the 23 chromosome pairs of PSCs. From Fig. 3 we can deduce that in PSCs, the chromatin state is not uniformly similar, with Oct4, Sox2 and Nanog promoting a more de-condensed-like state of chromatin in ch. 17, 19 and 22. Variability in the de-condensation states of the different chromosome pairs, provides a distinctive image of the chromatin conformation state of human embryonic pluripotent cells. Work is in progress in Maggioni et al (in preparation) to examine open chromatin by the enzyme DNaseI HS from ENCODE project (http://www.genome.gov/encode/) and quantify nucleosome and histone content on different cell types. The model proposed in Section 3.1 (the six helices model) has been implemented under Mathematica 9 and used to produce Fig. 4. From Fig. 4(a), we observe a limited number of solenoid layers for chromosomes 17, 19 and 22 which confirms the ratio we have found in Fig. 3. Finally, Fig. 4(b) shows the normalized total curvature over all the 23 chromosome pairs computed according to the solenoid model. Again chromosomes 17, 19 and 22 show lower values of normalized total curvature with respect to the other ones.

A comparison between the *six helices model* (see Section 3.1) and *torus model* (see Section 3.2) is reported in Table 2 in terms of normalized total curvature, normalized bending energy and total number of base pairs per turn. The torus model shows lower values of normalized total curvature and bending energy with respect to the six helices model. Information about the normalized total curvature and normalized bending energy is not available from biological experiments; thus it is difficult to say which model is better. Nevertheless, the six helices model is more flexible allowing an accurate description of each single nucleosome and linkers-DNA between nucleosomes and layers.

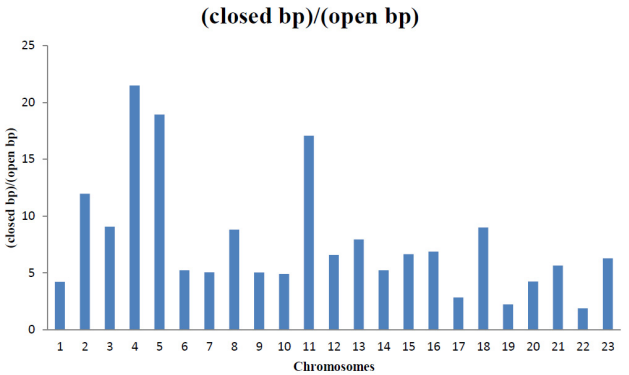

Fig. 3. Ratio between closed and open base pairs according to Oct4, Sox2 and Nanog binding regions over all the 23 chromosome pairs of human PSCs.

Table 2. Normalized total curvature, normalized bending energy and total number of base pairs per turn, respectively according to the *six helices model* (see Section 3.1) and *torus model* (see Section 3.2).

	$\mathcal{K}$ per turn	E_b per turn	*bp* per turn
Six helices model	76.97	7.61	1182
Torus model	75.43	5	1182

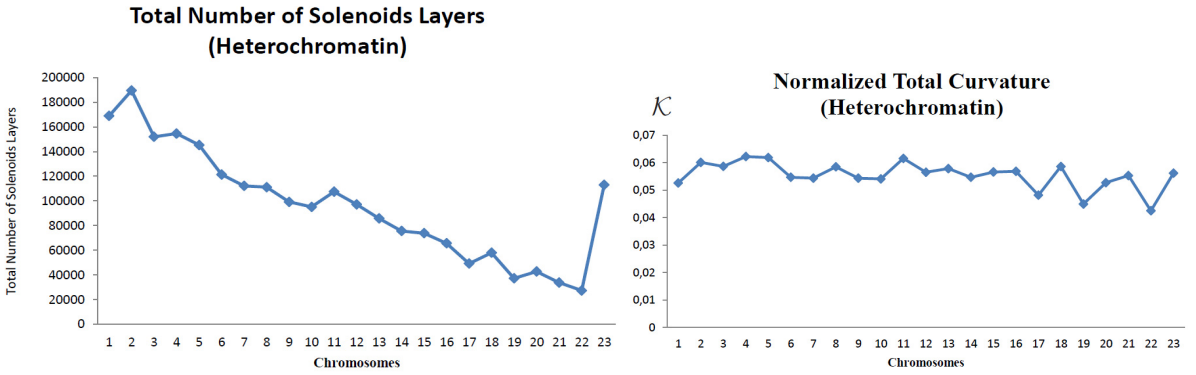

(a) (b)

Fig. 4. (a) Total number of solenoid layers, and (b) normalized total curvature over all the 23 chromosome pairs of PSCs.

5. Conclusions

Induced pluripotent cells hold great promise for regenerative medicine, like embryonic stem cells since they have the potential to generate all cells of the human body and therefore, can be utilized for cell or tissue replacement therapies. The iPSs are generated by chromatin remodeling of non-pluripotent cells, an epigenomic process that is still not completely characterized. The chromatin state of iPSCs is determined by local and global chromatin structural changes that are generated by transcription factor binding to particular regions of the chromosomes. The binding of the transcription factors initiates chromatin structural remodeling induced by epigenomic factors that have the capacity to modify histone proteins. Two geometric models for chromatin fibre conformation are presented and compared in terms of geometric quantities. The models are tested on ChIP Data generated from human pluripotent embryonic stem cells (PSCs) (Boyer et al., 2005). These models provide insight into the chromatin structural state of human pluripotent stem cells in terms of geometric spatial information.

We have found that in PSCs the chromatin state is not uniform for all the chromosomes, with Oct4, Sox2 and Nanog activity promoting more de-condensation of chromatin structure in certain chromosomes than in others, in particular on chromosomes 17, 19 and 22 (open state). These differences in chromosome geometry provide a deeper insight into processes associated with cellular reprogramming.

Future bio-mathematical-informatics modeling of chromosome structural states of particular cell types, is an important contribution for identifying epigenomic agents and mechanisms in regenerative medicine and disease models such as cancer and ailments associated with particular life style conditions, such as cardiovascular disease and diabetes (Kwa et al., 2011; Mosca et al., 2010; Milanesi, 2010).

Ongoing work in our laboratory by utilizing other approaches such “fingerprinting” chromatin regions accessible by DNaseI will allow us to define at higher resolution the structural chromatin state of specific cell types and the various transitional chromatin states during cellular reprogramming and disease. Additionally, future modeling will be correlated with induced changes in nucleosome and histone content in different cell states to obtain a better understanding of chromosome geometry and epigenomic processes.

Acknowledgements

FM would like to thank for the kind hospitality the Isaac Newton Institute for Mathematical Sciences Cambridge (UK), where this work was carried out during the program “Topological Dynamics in the Physical and Biological Sciences” (16 July - 21 December, 2012).

FM Grant support: CARIPLO foundation Grant 2012: “FYRE - Fostering Young Researchers project.”

ZI Grant support: the N.O.B.E.L. Grant and Cariplo-Progetti-Internazionali grant n. 2008-2015 from Fondazione-CARIPLO; the MIUR-FIRB grants RBAP11BYNP and RBAP11Z4Z9.

References

Maggioni, F. & Ricca, R.L. (2006) Writhing and coiling of closed filaments. *Proc Roy Soc A*, *462*, 3151 - 3166.
Ricca, R.L. & Maggioni, F. (2008) Multiple folding and packing in DNA modeling. *Comput. Math. Appl, 55*, 1044 - 1053.
Maggioni, F, Potra F & Bertocchi, M. (2013) Optimal kinematics of a looped filament. *J. Opt. Theory Appl*, 159(2) , 489 - 506.
Maggioni, F., Alamri, S., Barenghi, C.F. & Ricca R.L. (2013) Vortex knots dynamics in Euler fluids. *IUTAM Procedia*, Elsevier, 7, 29 - 38.
Călugăreanu, G. (1961) Sur les classes d'isotopie des nœuds tridimensionnels et leurs invariants. *Czechoslovak Math. J.*, *11*, 588 - 625.
White, J.H. (1969) Self-linking and the Gauss integral in higher dimensions. *Amer. J. Math.*, *91*, 693 - 728.
Fuller, F.B. (1971) The writhing number of a space curve. *Proc. Natl. Acad. Sci. U.S.A.*, *68*, 815 - 819.
Olins, D.E., & Olins, A.L. (2003) Chromatin history: Our view from the bridge. *Nature Reviews Molecular Cell Biology*, *4*, 809 - 814.
Finch, J.T. & Klug, A. (1976) Solenoidal model for superstructure in chromatin. *Proc. Natl. Acad. Sci. U. S. A*, *73*, 1897 - 1901.
Van Holde, K. and Zlatanova, J. (2007) Chromatin fibre structure: Where is the problem now? Semin. *Cell Dev. Biol.*, *18*, 651 - 658.
Tremethick,D.J. (2007) Higher-order structures of chromatin: the elusive 30 nm fibre. *Cell*, *128*, 651 - 654.
Dorigo, B., Schalch, T., Kulangara, A., Duda, S., Schroeder, R.R., & Richmond, T.J. (2004) Nucleosome arrays reveal the two-start organization of the chromatin fibre. *Science*, *306*, 1571 - 1573.
Schalch, T., Duda, S., Sargent, D.F., & Richmond, T.J. (2005) X-ray structure of a tetranucleosome and its implications for the chromatin fibre. *Nature*, *436*, 138 - 141.
Worcel, A., Strogatz, S., & Riley, D. (1981) Structure of chromatin and the linking number of DNA. *Proc. Natl. Acad. Sci. U. S. A.*, *78*, 1461 - 1465.
Beard, D.A. & Schlick, T. (2001a) Computational modeling predicts the structure and dynamics of chromatin fibre. *Structure, 9*, 105 - 114.
Beard, D.A. & Schlick, T. (2001b) Modeling salt-mediated electrostatics of macromolecules: The discrete surface charge optimization algorithm and its application to the nucleosome. *Biopolymers*, *58*, 106 - 115.
Beard, D.A. & Schlick, T. (2003) Unbiased rotational moves for rigid-body dynamics. *Biophys. J.*, *85*, 2973 - 2976.
Zhang, Q., Beard, D.A., & Schlick, T. (2003) Constructing irregular surfaces to enclose macromolecular complexes for mesoscale modeling using the Discrete Surface Charge Optimization (DiSCO) algorithm. *Journal of Computational Chemistry*, *24*, 2063 - 2074.
Sun, J., Zhang, Q., & Schlick, T. (2005) Electrostatic mechanism of nucleosomal array folding revealed by computer simulation. *Proc. Natl. Acad. Sci. U. S. A*, *102*, 8180 - 8185.
Schiessel, H. (2013) Biophysics for Beginners: A Journey Through the Cell Nucleus, Pan Stanford Publishing,
Rossetto V., & Everaers, R. (2005) Possible structures for the 30 nm chromatin fibre, to appear.
Woodcock, C.L., Grigoryev, A., Horowitz, R.A. & Whitaker, N. (1993) A chromatin folding model that incorporates linker variability generates fibres resembling the native structures. *Proc. Nat. Acad. Sci. USA, 90*, 9021 - 9025.
de Boor, C. (1978) *A practical guide to splines.* Applied Mathematical Sciences, Vol. 27, New York: Springer Verlag.
Maggioni, F., Bertocchi, M., Mosca, E., Reinbold, R. & Zucchi, I. Modeling chromatin fibre structure in cellular reprogramming of human cells. (in preparation).
Kauffman, L.H. (1997) Fourier Knots. arXiv:q-alg/9711013v2.
Boyer, Lee, T.I., Cole, M.F., Johnstone, S.E., Levine, S.S., Zucker, J.P., Guenther, M.G., Kumar, R.M., Murray, H.L., Jenner, R.G., Gifford,
Kim, J.B., Greber, B., Araúzo-Bravo M.J., Meyer J., In Park K., Zaehres H. & Schöler, H.R. (2009a) Direct reprogramming of human neural stem cells by *OCT4*. *Nature advance online publication*, doi:10.1038/nature08436.
Kim, J.B., Sebastiano, V., Wu, G., Araúzo-Bravo, M.J., Sasse, P., Gentile, L., Ko, K., Ruau, D., Ehrich, M., van den Boom, D., Meyer, J., Hübner, K., Bernemann, C., Ortmeier, C., Zenke, M., Fleischmann, B.K., Zaehres, H. & Schöler, H.R. (2009b) Oct4-induced pluripotency in adult neural stem cells. *Cell 136*, 411–419.
Takahashi, K. & Yamanaka, S. (2006) Induction of pluripotent stem cells from mouse embryonic and adult fibroblast cultures by defined factors. *Cell 126,* (4), 663–76. doi:10.1016/j.cell.2006.07.024. PMID 16904174.
Wernig, M; Meissner, A; Foreman, R; Brambrink, T; Ku, M; Hochedlinger, K, Bernstein, BE, & Jaenisch, R. (2007) In vitro reprogramming of fibroblasts into a pluripotent ES-cell-like state. *Nature 448,* (7151) 318–24. doi:10.1038/nature05944. PMID 17554336.
Zhou, T., Benda, C., Dunzinger, S., Huang, Y., Ho, J.C., Yang, J., Wang, Y., Zhang, Y., Zhuang, Q., Li, Y., Bao, X., Tse, H., Grillari, J., Grillari-Voglauer, R., Pei, D. & Esteban, M.A. (2012) Generation of human induced pluripotent stem cells from urine samples. *Nature Protocols 7,* (12), 2080–2089. doi:10.1038/nprot.2012.115.
Aoi, T., Yae, K., Nakagawa, M., Ichisaka, T., Okita, K., Takahashi, K., Chiba, T. & Yamanaka, S. (2008) Generation of Pluripotent Stem Cells from Adult Mouse Liver and Stomach Cells. *Science 321,* (5889), 699–702.
Melton, D.K., Jaenisch, R. & Young, R.A. (2005) Core Transcriptional Regulatory Circuitry in Human Embryonic Stem Cells. *Cell, 122*, 947 - 956.

Kwa, F.A., Balcerczyk, A., Licciardi, P., El-Osta, A., & Karagiannis, T.C. (2011) Chromatin modifying agents - the cutting edge of anticancer therapy. *Drug Discov Today, 16*, 543 - 547.
Mosca, E., Cocola, C., Sabour, D., Pelucchi, P., Bertalot, G., Palumbo, O., Carella, M., Götte M., Schöler, H.R., Reinbold, R., Zucchi, & I., Milanesi, L. (2010) Overlapping Genes May Control Reprogramming of Mouse Somatic Cells into Induced Pluripotent Stem Cells (iPSCs) and Breast Cancer Stem Cells. In *Silico Biol.*, *10*, 207 - 221.